Self-consistent calculations of depletion- and accumulation-layer profiles in n-type GaAs

D. H. Ehlers and D. L. Mills
Department of Physics, University of California, Irvine, California 92717
(Received 21 April 1986)

We present self-consistent calculations of depletion- and accumulation-layer profiles for a range of carrier concentrations in n-type GaAs, at room temperature. The Hartree approximation is used, with the self-consistent potential fitted in the end to the analytic form introduced earlier by Baraff and Appelbaum [Phys. Rev. B 5, 475 (1972)]. We compare these results to profiles obtained from the Thomas-Fermi approximation.

I. INTRODUCTION

Near the surface of a doped semiconductor, the carrier density often differs dramatically from that in the bulk. One may encounter depletion layers as thick as a few hundred angstroms, within which the free-carrier density drops dramatically below that in the bulk, or accumulation layers which contain an excess of carriers. Particularly intriguing are the very thin inversion layers created by application of a strong electric field in, for example, metal-oxide-semiconductor (MOS) devices. In an inversion layer, electrons are free to move parallel to the surface, but their motion normal to it is quantized, with the result that only one or a small number of subbands is occupied.

When only one subband is occupied in an inversion layer, we have a physical realization of a two-dimensional electron gas. In recent years, these systems have been extensively studied from both the theoretical and the experimental point of view.[1] On the theoretical side, we have self-consistent calculations of the charge profile in the inversion layer, studies of the electromagnetic response based on a proper nonlocal description of the electrons, and many other studies. Nonlocal analyses of the electromagnetic response are rendered quite tractable by the fact that only a small number of subbands are occupied. This has the consequence that the relevant integral equation has a kernel with a rather small number of terms, each separable in form. Finally, of course, we have the quantized Hall effect in such systems.

Less attention has been devoted recently to the theoretical study of depletion and accumulation layers, under conditions where an inversion layer is absent. Our attention has been attracted to such surfaces by the recent and very beautiful experimental studies by Matz and Lüth.[2] By means of electron energy-loss spectroscopy, these authors study surface plasmons on GaAs surfaces, in the presence of a depletion layer. In the method, surface plasmons are excited which have wave vectors parallel to the surface, $Q_{||}$, which satisfies $Q_{||}d \cong 1$, where d is the thickness of the depletion layer.[3] Thus, the spectra are influenced strongly by the presence of a depletion or accumulation layer and, in fact, after chemisorption of hydrogen on the surface the frequencies observed by Matz and Lüth were substantially lower than expected from the bulk carrier density, presumably because the depletion-layer profile is altered.

There have been theoretical studies of surface plasmons on model semiconductor surfaces which assume the material can be described by a *local* frequency-dependent dielectric function $\epsilon(z,\omega)$, with z the direction normal to the surface. The dependence on z arises from the free-carrier contribution

$$-4\pi n(z)e^2/m^*\omega^2 ,$$

with $n(z)$ the local electron density at point z. One may question the quantitative validity of such a model, since the thickness of the depletion or accumulation layer is typically comparable to the Thomas-Fermi screening length. Under these conditions, the amplitude of a charge fluctuation at z is not proportional to the electric field at this point, but rather to the average of the electric field over the whole depletion-layer region, as described by the appropriate nonlocal theory.

There is a particular problem with the description of depletion layers in such a model. The surface-plasmon frequency is necessarily lower than the bulk plasmon frequency where $\epsilon(\omega)$ vanishes. Since $n(z)$ drops to zero at the surface, necessarily there must be a point z_0, where $\epsilon(z_0,\omega_s)=0$, with ω_s the surface-plasmon frequency. There is a singularity in the electric field at this point[4] which is rather unphysical in our view.

We wish to construct a nonlocal description of surface plasmons in systems such as those just discussed. The first step is to construct a self-consistent description of the depletion- or accumulation-layer profile. The present paper discusses such a calculation, for a wide range of electron concentrations in n-type GaAs, and for a range of surface densities. We do this in the Hartree approximation, arguing below that exchange and correlation effects provide only modest corrections, in the parameter regime explored.

We have used a scheme introduced some years ago by Baraff and Appelbaum.[5] The idea is as follows. In all but the most heavily doped semiconductors well below room temperature, the electrons are at most partially degenerate. There are no Friedel oscillations, and the spatial variation of the electron density $n(z)$, and the subsequent self-consistent potential is quite smooth. Baraff and Ap-

pelbaum describe this smooth potential by a suitably placed Morse potential, with slope at the surface constrained by the value of the charge per unit area trapped on the surface. One may use a series method to obtain, very quickly, the single-particle states with a choice of the remaining parameters. With these, one calculates $V(z)$, the Hartree potential, and readjusts the parametrized Morse potential. In the end, one obtains a Hartree potential which is self-consistent, and fitted quite accurately by an analytic form, from which any desired solution to the Schrödinger equation may be obtained easily by a series method. The advantage to us is that certain Green's functions we require in our subsequent study of surface plasmons may be constructed from the appropriate series solutions, without the need to integrate a Schrödinger equation numerically.

Baraff and Appelbaum were interested in a fully degenerate gas of free carriers. Here we show how their scheme may be extended to an ensemble of free carriers that are only partially degenerate, or are possibly well described by Maxwell-Boltzmann statistics. Also, most of their numerical work explored the case where a magnetic field is present, which introduces Landau levels. We only consider the case of zero magnetic field, and provide Morse potential parameters which reproduce the self-consistent Hartree potential over a rather wide range of carrier densities, and surface charge densities, for GaAs at room temperature. We also compare our results with the description provided by the Thomas-Fermi model commonly employed in the description of depletion and accumulation layers.[6] We find the Thomas-Fermi description rather poor for most of the parameter range considered.

II. SELF-CONSISTENT DESCRIPTION OF THE CHARGE PROFILE

Ingredients of the basic model may be appreciated by considering two basic lengths which enter the problem. For free carriers of mass m^*, described by Maxwell-Boltzmann statistics, the de Broglie wavelength λ_T of a typical electron is

$$\lambda_T = 2\pi\hbar(3m^* k_B T)^{-1/2} .$$

For GaAs, $m^* = 0.069m$, with m the free-electron mass, and then $\lambda_T = 237$ Å at room temperature. There is also the Debye (or Thomas-Fermi) screening length,

$$\lambda_s = (\epsilon_s k_B T / 4\pi n e^2)^{1/2} ,$$

with n the free-carrier concentration, and ϵ_s the static dielectric constant. This length sets the thickness of a depletion or accumulation layer in the Thomas-Fermi approximation. For $n = 10^{17}$ cm^{-3}, after using $\epsilon_s = 12.9$, we have $\lambda_s \cong 136$ Å.

These lengths are sufficiently long compared to a lattice constant that we may average over microscopic details. We regard the ionized donors as a positively charged background, smeared out in the manner familiar from the jellium model of metals. We also require the free-carrier wave functions to vanish at the surface, and ignore the small tail which leaks out into the vacuum.

Before we begin, we note that the lengths estimated above show that the Thomas-Fermi[6] description of the depletion or accumulation layer is expected to be poor, and a quantum-mechanical treatment is required. The Thomas-Fermi picture assumes $\lambda_T \ll \lambda_s$, an inequality satisfied nowhere in the carrier density range considered here. Stahl has presented a treatment of surface plasmons in the presence of a depletion layer,[7] treating the electrons in the infinite barrier model, with the single-particle wave functions pure sinusoids with a zero at the surface. In essence, this picture implicitly assumes $\lambda_T \gg \lambda_s$, so the range of wavelengths available in the thermal sea of electrons is insufficient to form a depletion or accumulation layer as thin as λ_s. Clearly, we are in the regime where $\lambda_T \sim \lambda_s$, and neither extreme is realized.

The single-particle wave functions are then solutions of

$$\left[-\frac{\hbar^2}{2m^*}\nabla^2 + V(z) \right] \psi_\alpha(\mathbf{r}) = E_\alpha \psi_\alpha(\mathbf{r}) , \tag{2.1}$$

with $V(z)$ the self-consistent potential constructed as described below. The wave vector $\mathbf{k}_{||}$ parallel to the surface is a good quantum number, the index α is replaced by the combination $(\mathbf{k}_{||} i)$, where i labels the particular solution of wave vector $\mathbf{k}_{||}$ under consideration. If A is the area of the sample, we have solutions of the form

$$\psi_{\mathbf{k}_{||},i}(\mathbf{r}) = \frac{e^{i\mathbf{k}_{||}\cdot\mathbf{r}_{||}}}{\sqrt{A}} \chi_i(z) , \tag{2.2}$$

where, with $E_{\mathbf{k}_{||},i} = (\hbar^2 k_{||}^2 / 2m^*) + \varepsilon_i$ we have

$$\left[-\frac{\hbar^2}{2m^*}\frac{d^2}{dz^2} + V(z) \right] \chi_i(z) = \varepsilon_i \chi_i(z) . \tag{2.3}$$

Following Baraff and Appelbaum, we introduce a quantization length L in the direction normal to the surface, and for $\chi_i(z)$ we have the boundary conditions

$$\chi_i(0) = 0 , \tag{2.4a}$$

$$\chi_i(L) = 0 . \tag{2.4b}$$

In the end, we shall let $L \to \infty$, focusing our attention on the near vicinity of the surface $z = 0$.

In the spirit of the local density approximation to the density functional formalism, $V(z)$ is to be the Hartree potential supplemented by an exchange and correlation potential, V_{xc}. We are handicapped, in that in the regime of interest, where the free carriers are nondegenerate or at most partially degenerate, we have no analytic form for V_{xc}, or interpolation formulas similar to those used in the description of the fully degenerate electron gas. Numerical studies, based on the ring-diagram approximation are available, as are analytic formulas valid in the high-temperature limit.[8] In Sec. III, we examine these and argue that in the range of carrier concentration of interest to us, exchange and correlation corrections are modest compared to the Hartree contribution which dominates. Thus, following Baraff and Appelbaum again, we confine our attention to the Hartree approximation.

We then replace $V(z)$ by $-e\Phi(z)$, where $\Phi(z)$ is the electrostatic potential which emerges as the solution of the Poisson equation

$$\frac{d^2}{dz^2}\Phi(z)=\frac{4\pi e}{\epsilon_s}\delta n(z) , \tag{2.5}$$

where ϵ_s again is the static dielectric constant, and $\delta n(z)$ is the deviation of electron density from its bulk value. The zero of energy is chosen as the bottom of the conduction band in the bulk of the crystal, so as $z\rightarrow\infty$, $\Phi(z)\rightarrow 0$.

There are two contributions to $\delta n(z)$, so we write $\delta n(z)=\delta n_c(z)+\delta n_D(z)$. The first is from the free carriers in the conduction band, and if $f(x)=(e^{\beta x}+1)^{-1}$ is the Fermi-Dirac function with $\beta=(k_BT)^{-1}$, and n_0 is the bulk free-carrier concentration, we have

$$\delta n_c(z)=\frac{2}{(2\pi)^2}\int d^2k_{\parallel}\sum_i f\left[\frac{\hbar^2k_{\parallel}^2}{2m^*}+\epsilon_i-\mu\right]\chi_i^2(z)-n_0 . \tag{2.6}$$

The second has its origin in the fact that the donor binding energy is shifted from the bulk value E_D to $E_D-e\Phi(z)$, by virtue of the potential $\Phi(z)$. The concentration of ionized donors near the surface thus differs from that in the bulk, and if n_D is the concentration of donor impurities, with

$$[1-f(E_D-\mu)]$$

the fraction of these which are ionized, we have

$$\delta n_D(z)=n_D[f(E_D-e\Phi(z)-\mu)-f(E_D-\mu)] . \tag{2.7}$$

In our numerical work, we calculate E_D from the hydrogenic model. The deviation $\delta n_D(z)$ in the ionized donor concentration influences the results significantly only at the highest concentrations we consider in our calculations.

In what follows, for the remainder of the paper, we measure all energies in units of k_BT, so, for example, $-e\Phi(z)$ is replaced by $k_BT\phi(z)$, where ϕ is dimensionless. We also measure lengths in terms of the thermal wavelength

$$\lambda=(\hbar^2/2m^*k_BT)^{1/2} ,$$

which assumes the value 46.2 Å for GaAs at room temperature. This is not the wavelength of an electron with kinetic energy $\frac{3}{2}k_BT$, but proves to be a convenient scaling length. We then replace z by λy, wave vectors such as $k_{\parallel}$ by $\lambda^{-1}\kappa_{\parallel}$, and wave functions χ_i by $\chi_i\lambda^{-1/2}$. The Schrödinger equation then becomes

$$\left[-\frac{d^2}{dy^2}+\phi(y)\right]\chi_i(y)=\epsilon_i\chi_i(y) , \tag{2.8}$$

with all quantities dimensionless, and then Poisson's equation is

$$\frac{d^2\phi}{dy^2}=-8\pi\frac{\lambda}{a_0}\delta n(y) , \tag{2.9}$$

where $a_0=\epsilon_s\hbar^2/m^*e^2$ is the Bohr radius.

The electric field at the surface $(d\phi/dy)_{0+}$ is found by integrating Poisson's equation,

$$\left[\frac{d\phi}{dy}\right]_{y=0+}=-8\pi\frac{\lambda}{a_0}Q , \tag{2.10}$$

where

$$Q=-\int_0^{\infty}dy\,\delta n(y) \tag{2.11}$$

is the charge displaced by virtue of the presence of a depletion layer, or an accumulation layer. Considerations of electrical neutrality require that $-Q$ equal Q_s, the (dimensionless) charge per unit area trapped on the surface, or Q might be controlled by an external electric field. Also, the electrostatic potential may be obtained by integrating Eq. (2.9), noting the boundary conditions

$$\phi(y)=-\frac{8\pi\lambda}{a_0}\int_0^{\infty}y'\,\delta n(y+y')dy' . \tag{2.12}$$

We now focus on the contributions to the electron density in the conduction band, $\delta n_c(y)$. We have contributions from bound states, for which $\epsilon_i<0$, and mobile electrons with $\epsilon_i=\kappa_i^2\geq 0$. The wave functions of the latter have the form

$$\chi_i(y)=C(\kappa_i)g(\kappa_i,y)\sin[\kappa_iy+\eta(\kappa_i)] . \tag{2.13a}$$

Here $C(\kappa_i)$ is the normalization constant, and as $y\rightarrow\infty$, $g(\kappa_i,y)\rightarrow 1$. This provides the proper behavior as $y\rightarrow\infty$. The boundary condition in Eq. (2.4a) can be satisfied by choosing the phase shift $\eta(\kappa_i)$ appropriately, as one sees from Ref. 5 and the discussion in Appendix A, while Eq. (2.4b) requires

$$\kappa_iL+\eta(\kappa_i)=(m+i)\pi . \tag{2.13b}$$

In converting the sum on i to an integration, of course we retain the sum over the bound states, henceforth denoted by the index n, and the sum over the continuum is dealt with through the prescription[5]

$$\sum_i\rightarrow\int_0^{\infty}d\kappa\frac{1}{(\Delta\kappa/\Delta i)}=\int_0^{\infty}\frac{d\kappa}{\pi}\left[L+\frac{d\eta}{d\kappa}\right]$$
$$=\frac{2}{\pi}\int_0^{\infty}d\kappa\frac{1}{C^2(\kappa)} , \tag{2.14}$$

so that

$$\delta n_c(y)=\int\frac{d^2\kappa_{\parallel}}{2\pi^2}\left[\sum_n f(\epsilon_n+\kappa_{\parallel}^2-\mu)\chi_n^2(y)+\int_0^{\infty}d\kappa\frac{2}{\pi C^2(\kappa)}f(\kappa^2+\kappa_{\parallel}^2-\mu)\chi_\kappa^2(y)\right]-n_0 , \tag{2.15}$$

where in Eq. (2.15) and in what follows, after converting to dimensionless units, $f(x)=(e^x+1)^{-1}$.

The chemical potential μ is found from

$$n_0=\frac{1}{4\pi^3}\int d^3\kappa f(\kappa^2-\mu)\ , \tag{2.16}$$

which allows Eq. (2.15) to be rewritten

$$\delta n_c(y)=\int\frac{d^2\kappa_{||}}{2\pi^2}\left[\sum_n f(\varepsilon_n+\kappa_{||}^2-\mu)\chi_n^2(y)+\int_0^\infty\frac{d\kappa}{\pi}f(\kappa^2+\kappa_{||}^2-\mu)\times\left[2\frac{\chi_\kappa^2(y)}{C^2(\kappa)}-1\right]\right]. \tag{2.17a}$$

For large y, the bound-state contribution has decayed to zero, and we are left with only asymptotic contributions from the continuum.

In the Thomas-Fermi approximation, incidentally, one replaces $\delta n_c(y)$ by

$$\delta n_{\rm TF}(y)=\int\frac{d^3\kappa}{4\pi^3}f[\kappa^2+\phi(y)-\mu]-n_0\ . \tag{2.17b}$$

Instead of solving Eqs. (2.8), (2.12), and (2.17a) self-consistently, we adopt the procedure used in Ref. 5. A parametrized potential is employed in the Schrödinger equation, which may then be solved straightforwardly by a series approach. Then $\delta n(y)$ may be constructed from these solutions, and finally the potential $\phi(y)$, and new parameters are chosen for the parametrized potential. The form of the parametrized potential introduced in Ref. 5 is of the Morse form

$$\phi_p(y)=\frac{V_0}{1-\beta}(e^{-\mu y}-\beta e^{-2\mu y})\ , \tag{2.18}$$

where the value of the parameter β is constrained by the boundary condition in Eq. (2.10),

$$\beta=1-\frac{1}{2-8\pi(\lambda/a_0)(Q/V_0\mu)}\ . \tag{2.19}$$

The potential depth V_0 at $z=0$ is determined by an iteration scheme, i.e., given an initial V_0, one calculates $\phi(0)$, and a linear combination of the initial V_0 and $\phi(0)$ is chosen as the next guess for V_0. This continues until $\phi(0)$ and V_0 agree. At each iteration step, once a value for V_0 is chosen, the parameter μ is adjusted so that the condition of charge neutrality in Eq. (2.11) is obeyed.

There will, of course, always be some discrepancy between the best parametrized potential and the Hartree potential generated by the charge density generated by the optimum parametrized potential. An attractive feature of the scheme is, however, that strict charge neutrality is maintained.

In Appendix A, we discuss the solution of the Schrödinger equation with the parametrized potential $\phi_p(y)$, and the boundary conditions in Eq. (2.4). Using these wave functions, and forming $\delta n_c(y)$, real-space integrations must be carried out to compute Q and $\phi(y)$. These may be performed analytically, as discussed in Appendix B. This may be done with no special assumption about the degree of degeneracy present, i.e., we may perform these integrals with the full general form of the Fermi-Dirac function in $\delta n_c(y)$. Then the only integral that must be evaluated on the computer is that over the wave vector κ of the mobile states, as indicated in Eqs. (B14) and (B15). While in the end, the parametrized potential can differ somewhat from the full self-consistent form, the scheme works remarkably well in our view, and the amount of computing power required to complete the finite temperature calculation is rather modest. For a given carrier density, and a given choice of the surface charge Q, determination of the optimum parametrized potential $\phi_p(y)$ typically requires less than three minutes of CPU (central processing unit) time on a Digitial Equipment Corporation VAX11/780 minicomputer.

III. DISCUSSION AND RESULTS

In Fig. 1, various parameters which emerge from the analysis are plotted against the (dimensionless) charge per unit area trapped on the surface. When $Q=0.1$, the maximum value considered, there is $0.1e$ in an area of size λ^2, corresponding to an actual surface charge density of $4.7\times10^{11}e/\text{cm}^2$. In each figure, the horizontal dotted-dashed line is the Fermi energy, and the solid line is the value of the parametrized potential at the surface, in units of k_BT. For comparison, we show the surface potential calculated in the Thomas-Fermi approximation in the dotted line. We show also the values of the parameter $1/\mu$, which is a measure of the thickness of the depletion or accumulation layer in units of λ. In each figure, there is a region of surface charge densities where we cannot find meaningful values of μ. For large, positive Q, we have a depletion layer, and the potential decreases monotonically to zero. As Q is decreased, at some point the potential develops an attractive well; this happens for positive Q, when $\phi(0)$ is positive. The scheme breaks down just as the potential first crosses zero, to form the attractive well.

It is clear from Fig. 1 that the Thomas-Fermi model is of limited quantitative validity, most particularly in the accumulation-layer region $Q<0$, though it does reproduce the surface potential well for large positive Q. Notice that the "flat band configuration" (by definition the point where the surface potential vanishes) occurs not at $Q=0$, as it does in the Thomas-Fermi approximation, but at a positive value of Q. When $Q=0$, there is necessarily a dipole layer present, with a sign such that the surface potential is depressed below the bulk value. Since the wave functions of all electrons drop to zero at the surface, there is a deficit of charge in a layer with thickness of roughly λ, and this must be compensated by a pileup of excess charges a bit farther into the crystal. We shall discuss these charge distributions shortly.

Note that the full theory does not result in a simple shift of the Q scale for the self-consistent potential, as can be seen in Fig. 1. The surface potential $\phi(0)$ changes more strongly with Q in the full theory, when compared

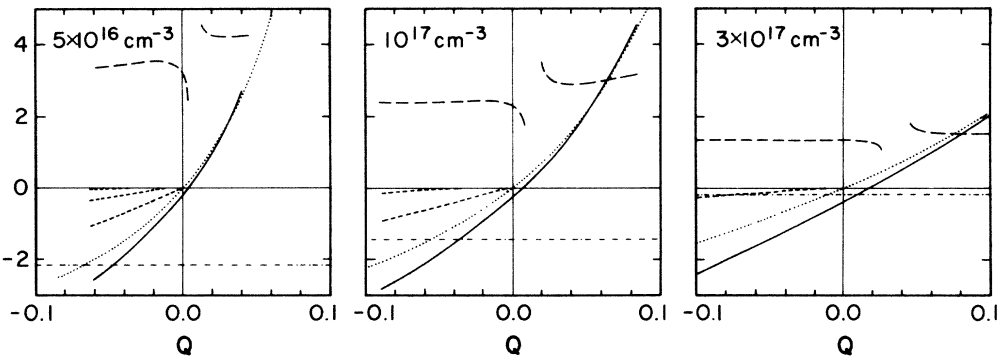

FIG. 1. For the three bulk carrier concentrations indicated, we summarize parameters which emerge from the analysis. The horizontal dotted-dashed line is the Fermi energy, and the solid lines give values for the surface potential in units of k_BT. The dotted lines are the Thomas-Fermi values of the surface potential. We show μ^{-1} (in units of λ) by broken lines (long dashed), and the energies of the bound states by dashed lines.

to the Thomas-Fermi results. In the limit of a strong depletion layer, the error produced in the Thomas-Fermi picture by overlooking the influence of the surface boundary condition on the electron wave functions has less influence, simply because the presence of the repulsive surface produces, in the Thomas-Fermi picture, a deficit of charge near the surface which mimics that introduced by the boundary condition in the full theory. In contrast, the error is appreciable for the accumulation layer. A proper treatment of the bound states is found to be important here.

We can now assess the importance of the exchange and correlation effects neglected in the calculation. As remarked earlier, we do not have in hand simple analytic or empirical expressions for these energies, as in the case of the degenerate electron gas. However, Gupta and Rajagopal[8] give simple expressions for the exchange and correlation energy in the limit

$$t = T/T_F = (3\pi^2 n)^{-2/3} \gg 1 ,$$

where in the last statement n is our dimensionless electron density, equal to the number of electrons in the volume λ^3. For the exchange energy, when $t \gg 1$ we have

$$V_x = -4\pi \frac{\lambda}{a_0} n \tag{3.1a}$$

while the correlation energy V_c may be written

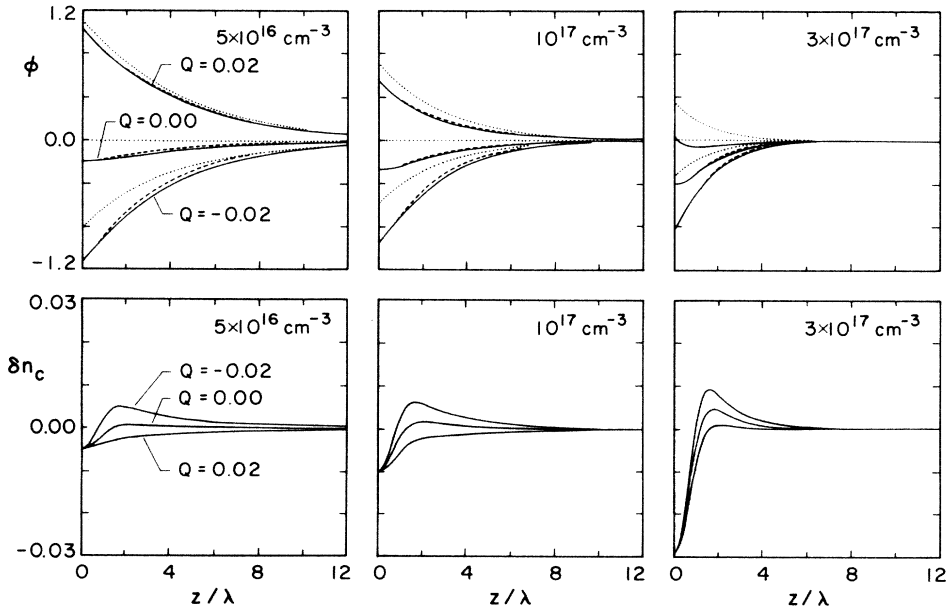

FIG. 2. For the three bulk carriers concentrations in Fig. 1, in the upper row we show the spatial variation of the potential, for three selected values of Q. The solid line is the parametrized potential, the dashed line is the Hartree potential generated from the charge density associated with the parametrized potential, and the dotted line is the Thomas-Fermi potential. The conduction electron densities $\delta n_c(y)$, for the same values of n_0 and Q, are shown in the lower row.

$$V_c = -\frac{\lambda}{a_0} | V_x |^{1/2} . \quad (3.1b)$$

Energies are again measured in units of $k_B T$. At room temperature, these expressions actually overestimate the energies for electron densities equal to or greater than 10^{17} cm^{-3}, if one compares them with the full calculations presented in Ref. 8. For $n = 10^{17}$ cm^{-3}, we have $t = 2.27$ at room temperature, and from Eq. (3.1) one estimates $V_x \cong -0.058$, $V_c \cong -0.112$. The exchange and correlation effects are thus of the order of 10% or less, for the parameter range covered in Fig. 1, if we compare with values of $\phi(0)$.

In Fig. 2, for three values of n_0 and Q, we show the spatial variation of the potential, and the conduction electron charge distribution. In the illustrations of the potentials (upper row), the solid line is the parametrized form, and the dashed line is the Hartree potential generated by the charge density associated with the parametrized potential. The two agree quite well for all cases. The dotted line is the Thomas-Fermi potential and we see that it provides a rather poor fit. The electron densities in the conduction band, δn_c, are illustrated in the lower row of Fig. 2. In contrast to these profiles the electron densities generated by the Thomas-Fermi picture all exhibit a monotonic variation with position, and in fact remain finite right up to the surface, a behavior inconsistent with the boundary condition applicable to the electron wave functions, as remarked above.

For the same surface charges, $Q = \pm 0.02$, the profiles of ϕ and δn_c are not only more extended at low carrier concentrations, as can be seen as well from the plots of $(1/\mu)$ in Fig. 1, but the screening requires greater absolute values of the surface potential $\phi(0)$ too.

The situation is somewhat different when Q is close to zero. The potential $\phi(0)$, the bound-state energy, and the parameter $(1/\mu)$ for $Q = 0$ are given in Fig. 3, over a wide range of bulk carrier concentrations. Here, $\phi(0)$ decreases with decreasing carrier concentration, while $(1/\mu)$ increases sharply thus still permitting a bound state with increasing energy for $n_0 \leq 2 \times 10^{17}$ cm^{-3}. This contrast between the cases of finite and zero surface charge shows that as the carrier concentration changes, there is no simple scaling with Q.

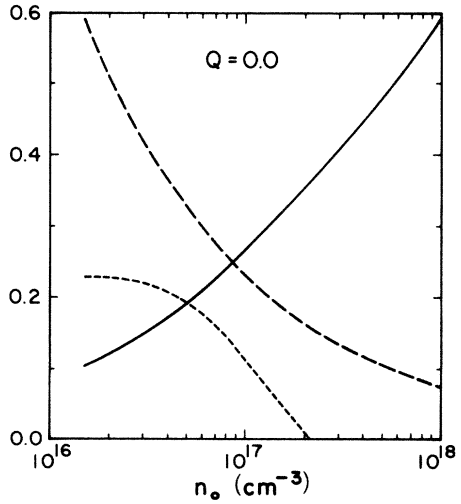

FIG. 3. For the case $Q = 0$ we give the variation with carrier concentration of the parameters $\phi(0)$ (in units of $k_B T$, solid line) and μ^{-1} (in units of 10λ, broken line), along with the bound-state energy ε_B (in $0.1 k_B T$, dashed line).

In conclusion, we have extended the calculation of Baraff and Appelbaum to the case where the free carriers are nondegenerate, and we find it possible to generate a parametrized potential that closely matches the self-consistent Hartree potential generated by depletion or accumulation layers in n-type GaAs. This may be done with a modest expenditure of computer time.

ACKNOWLEDGMENTS

This research was supported by U.S. National Aeronautics and Space Administration (NASA), through Grant No. NAG 3-679. One of us (D.H.E.) acknowledges financial support from the German Academic Exchange Service [Deutscher Akademischer Austauschdienst (DAAD)], Bonn, Germany.

APPENDIX A: SOLUTION OF THE SCHRÖDINGER EQUATION WITH THE PARAMETRIZED POTENTIAL

We consider solutions of

$$\left[-\frac{d^2}{dy^2} + \frac{V_0}{(1-\beta)} (e^{-\mu y} - \beta e^{-2\mu y}) - \varepsilon \right] \xi_\kappa(y) = 0 , \quad (A1)$$

where $\varepsilon = \kappa^2$. The equation admits a series solution of the form

$$\xi_\kappa(y) = e^{i[\kappa y + \eta(\kappa)]} \sum_{m=0}^{\infty} b_m(\kappa) e^{-m\mu y} , \quad (A2)$$

where

$$b_0(\kappa) = 1 , \quad (A3a)$$

$$b_1(\kappa) = \frac{V_0}{(1-\beta)} \frac{1}{\mu^2 - 2i\mu\kappa} , \quad (A3b)$$

and for $m \geq 2$,

$$b_m(\kappa) = \frac{V_0}{(1-\beta)} \frac{(b_{m-1} - \beta b_{m-2})}{m\mu(m\mu - 2i\kappa)} . \quad (A3c)$$

For bound states, $\chi_\kappa(y) = C(\kappa)\xi_\kappa(y)$, and then one lets $\kappa = ik_n$. As $y \to \infty$, for any choice of k_n, $\lim_{y\to\infty} \xi_{ik_n} = 0$. The allowed values of k_n are then determined by the boundary condition in Eq. (2.4a), which requires

$$\sum_{m=0}^{\infty} b_m(ik_n) = 0 , \quad (A4)$$

and the normalization constants are

$$C(ik_n) = \left[\sum_{r=0}^{\infty} \sum_{s=0}^{\infty} \frac{b_r b_s}{(r+s)\mu + 2k_n} \right]^{-(1/2)} . \quad (A5)$$

For the mobile states, we consider

$$\chi_\kappa(y) = C(\kappa) \mathrm{Im}[\xi_\kappa(y)] , \quad (A6)$$

which as $y \to \infty$ approaches

$$C(\kappa)\sin[\kappa y+\eta(\kappa)] .$$

The boundary condition is satisfied at $y=0$ if, once κ is selected, we choose $\eta(\kappa)$ such that

$$\sum_{m=0}^{\infty} b_m(\kappa)=Ae^{-i\eta(\kappa)} , \tag{A7}$$

where A is a real number. Levinson's theorem requires that $\eta(\kappa=0)=\pi M$, where M is the number of bound states. Since $\eta(\kappa)$ is a continuous function of κ, and $\eta(0)$ is known once the number of bound states is enumerated, we have a determination of $\eta(\kappa)$.

In practice, for the parameters we have explored, we find that 10 to 20 terms in Eq. (A2) prove adequate for an accurate calculation of the wave functions.

APPENDIX B: REAL-SPACE INTEGRALS REQUIRED IN THE ITERATION SCHEME

We begin with the contribution from the mobile carriers to the total screening charge Q, given in Eq. (2.11). We integrate from $y=0$, to some value R small compared to L (the limit $L \to \infty$ is implied). Then we have

$$Q_{\rm mob}=\frac{1}{2\pi^2}\int d^2\kappa_{||}\int_0^{\infty}\frac{d\kappa}{\pi}f(\kappa^2+\kappa_{||}^2-\mu)q_{\rm mob}(\kappa) ,$$

where

$$q_{\rm mob}(\kappa)=-\int_0^R\left[2\frac{\chi_\kappa^2(y)}{C^2(\kappa)}-1\right]dy$$
$$=-\frac{d\eta}{d\kappa}+\frac{\sin[2(\kappa R+\eta)]}{2\kappa} . \tag{B1}$$

The expression for $q_{\rm mob}(\kappa)$ is derived in Ref. 5. We turn to the remaining integrals shortly.

To calculate the electrostatic potential, we need

$$\delta n_{\rm mob}(\kappa,y)=2\frac{\chi_\kappa^2(y)}{C^2(\kappa)}-1$$
$$=-\cos[2(\kappa y+\eta)]+\sum_{m=1}^{\infty}e^{-m\mu y}\{A_m(\kappa)+\sin[2(\kappa y+\eta)]B_m(\kappa)-\cos[2(\kappa y+\eta)]D_m(\kappa)\} , \tag{B2}$$

where we break the expansion coefficients given in Appendix A into real and imaginary parts,

$$b_m(\kappa)=X_m(\kappa)+iY_m(\kappa) \tag{B3}$$

and then

$$A_m(\kappa)=2X_m+\sum_{s=1}^{m-1}(Y_{m-s}Y_s+X_{m-s}X_s) , \tag{B4a}$$

$$B_m(\kappa)=2Y_m+2\sum_{s=1}^{m-1}Y_{m-s}X_s , \tag{B4b}$$

and

$$D_m(\kappa)=-2X_m+\sum_{s=1}^{m-1}(Y_{m-s}Y_s-X_{m-s}X_s) . \tag{B4c}$$

We find that the mobile state contribution to the potential can then be written

$$\phi_{\rm mob}(y)=\frac{1}{2\pi^2}\int d^2\kappa_{||}\int_0^{\infty}\frac{d\kappa}{\pi}f(\kappa^2+\kappa_{||}^2-\mu)\varphi_{\rm mob}(\kappa,z) , \tag{B5}$$

where

$$\varphi_{\rm mob}(\kappa,y)=-\frac{8\pi\lambda}{a_0}\int_0^R y'\delta n_{\rm mob}(\kappa,y+y')dy'$$
$$=\frac{2\pi\lambda}{\kappa^2 a_0}[(\cos\{2[\kappa(R+y)+\eta]\}+2\kappa R\sin\{2[\kappa(R+y)+\eta]\}-\cos[2(\kappa y+\eta)])-4\kappa^2 h(\kappa,y)] , \tag{B6}$$

with

$$h(\kappa,y)=\sum_{m=1}^{\infty}\left[\frac{A_m(\kappa)}{m^2\mu^2}+\frac{B_m(\kappa)}{(m^2\mu^2+4\kappa^2)^2}\{4m\kappa\mu\cos[2(\kappa y+\eta)]+(m^2\mu^2-4\kappa^2)\sin[2(\kappa y+\eta)]\}\right.$$
$$\left.+\frac{D_m(\kappa)}{(m^2\mu^2+4\kappa^2)^2}\{(m^2\mu^2-4\kappa^2)\cos[2(\kappa y+\eta)]-4m\kappa\mu\sin[2(\kappa y+\eta)]\}\right]e^{-m\mu y} . \tag{B7}$$

In the integrals above, the limit $R\to\infty$ can be taken only after the integration on κ is performed. Note that

$$\int d^2\kappa_{||} f(\kappa^2+\kappa_{||}^2-\mu)=\pi\ln[1+\exp(\mu-\kappa^2)]\ . \tag{B8}$$

We are then left with the integral on κ in both Eqs. (B1) and (B5). These are evaluated by the method in Ref. 5. As $R\to\infty$, the oscillatory character of the integrand ensures that the dominant contributions come from the near vicinity of $\kappa=0$. Then in this region, we may replace $\eta(\kappa)$ by $\eta(0)+(d\eta/d\kappa)_0\kappa$, where Levinson's theorem requires $\eta(0)$ to be $M\pi$, with M the number of bound states. Then through a sequence of partial integrations one finds

$$\lim_{R\to\infty}\int_0^\infty \frac{d\kappa}{\pi}\ln(1+e^{\mu-\kappa^2})\frac{\sin[2(\kappa R+\eta)]}{2\kappa}=\tfrac{1}{4}\ln(1+e^{\mu})\ , \tag{B9}$$

and

$$\lim_{R\to\infty}\int_0^\infty \frac{d\kappa}{\pi}\ln(1+e^{\mu-\kappa^2})\frac{1}{\kappa^2}(\cos\{2[\kappa(R+y)+\eta]\}+2\kappa R\sin\{2[\kappa(R+y)+\eta]\}-\cos[2(\kappa y+\eta)]) \tag{B10}$$

$$=-\left[\left.\frac{d\eta}{d\kappa}\right|_0+y\right]\ln(1+e^{\mu})+\int_0^\infty\frac{d\kappa}{\pi}\left[\frac{2}{\kappa}\left[\frac{d\eta}{d\kappa}+y\right]\ln(1+e^{\mu-\kappa^2})\sin[2(\kappa y+\eta)]+\frac{2}{e^{\kappa^2-\mu}+1}\cos[2(\kappa y+\eta)]\right]\ . \tag{B11}$$

We now summarize the expressions for the various quantities we have used in the self-consistent calculation,

$$\delta n(y)=\delta n_D(y)+\frac{1}{2\pi}\left[\sum_n\ln(1+e^{\mu+k_n^2})\chi_n^2(y)+\int_0^\infty\frac{d\kappa}{\pi}\ln(1+e^{\mu-\kappa^2})\delta n_{\rm mob}(\kappa,y)\right]\ , \tag{B12}$$

where

$$\chi_n^2(y)=C^2(ik_n)\sum_{r=0}^{\infty}\sum_{s=0}^{\infty}b_r(ik_n)b_s(ik_n)e^{-[2k_n+(r+s)\mu]y} \tag{B13a}$$

and

$$\delta n_D(y)=n_0\frac{1-e^{\phi_p(y)}}{e^{E_D+\phi_p(y)-\mu}+1}\ , \tag{B13b}$$

and $\delta n_{\rm mob}(\kappa,y)$ given by Eq. (B2). In Eq. (B13b), n_0 is the bulk density of electrons in the conduction band, related to the density of donors n_D by

$$n_0=n_D[1-f(E_D-\mu)]$$

and

$$E_D=-(\lambda^2/a_0^2)\ .$$

Then

$$Q=-\frac{1}{2\pi}\left[\sum_n\ln(1+e^{\mu+k_n^2})-\tfrac{1}{4}\ln(1+e^{\mu})+\int_0^\infty\frac{d\kappa}{\pi}\frac{d\eta}{d\kappa}\ln(1+e^{\mu-\kappa^2})\right]-\int_0^\infty dy\,\delta n_D(y)\ , \tag{B14}$$

and for the potential,

$$\phi(y)=-4\frac{\lambda}{a_0}\left[\sum_n\left[\ln(1+e^{\mu+k_n^2})C^2(ik_n)\sum_{r,s=0}^{\infty}\frac{b_r(ik_n)b_s(ik_n)}{[2k_n+(r+s)\mu]^2}e^{-[2k_n+(r+s)\mu]y}\right]\right.$$

$$+\int_0^\infty\frac{d\kappa}{\pi}\left\{\ln(1+e^{\mu-\kappa^2})\left[h(\kappa,y)-\frac{1}{2\kappa}\left[\frac{d\eta}{d\kappa}+y\right]\sin[2(\kappa y+\eta)]\right]\right.$$

$$\left.\left.-\frac{1}{2}\frac{1}{e^{\kappa^2-\mu}+1}\cos[2(\kappa y+\eta)]\right\}+\tfrac{1}{4}\left[\left.\frac{d\eta}{d\kappa}\right|_0+y\right]\ln(1+e^{\mu})+2\pi\int_0^\infty y'\delta n_D(y+y')dy'\right]\ . \tag{B15}$$

[1]T. Ando, A. B. Fowler, and F. Stern, Rev. Mod. Phys. **54**, 437 (1982).

[2]R. Matz and H. Lüth, Phys. Rev. Lett. **46**, 500 (1981).

[3]See the discussion in Chap. 3 of H. Ibach and D. L. Mills, *Electron Energy Loss Spectroscopy and Surface Vibrations,* (Academic, San Francisco, 1982). The relevant remarks begin on p. 83.

[4]For an example of the field singularity, see Fig. 3 of S. L. Cunningham, A. A. Maradudin, and R. F. Wallis, Phys. Rev. B **10**, 3342 (1974).

[5]G. A. Baraff and J. A. Appelbaum, Phys. Rev. B **5**, 475 (1972).

[6]See the discussion which begins on p. 489 of J. P. McKelvey, *Solid State and Semiconductor Physics,* (Harper and Row, New York, 1966).

[7]A. Stahl, Surf. Sci. **134**, 297 (1983).

[8]U. Gupta and A. K. Rajagopal, Phys. Rep. **87**, 259 (1982).